er in the same lineage because both are mechanisms to avoid inbreeding. The obvious corollary, that gender dimorphism is more likely to evolve in groups that are self-compatible, has often been discussed (*9, 10, 20*). Yet, if scenarios like that proposed here are common, gender dimorphism may frequently evolve in lineages with self-incompatibility without negating inbreeding avoidance as a selective mechanism. The pathway presented here reinforces the importance of inbreeding avoidance in the evolution of gender dimorphism and could explain why a negative association between gender dimorphism and self-incompatibility has been difficult to find (*10*). Although gender dimorphism has been widely studied, many aspects are not fully understood, and new scenarios, such as the one presented here, surely await discovery.

References and Notes

1. E. L. Charnov, J. Maynard Smith, J. J. Bull, *Nature* **263**, 125 (1976).
2. J. R. Kohn, *Nature* **335**, 431 (1988).
3. M. A. Geber, T. E. Dawson, L. F. Delph, Eds., *Gender and Sexual Dimorphism in Flowering Plants* (Springer-Verlag, Berlin, 1999).
4. K. S. Bawa, *Annu. Rev. Ecol. Syst.* **11**, 15 (1980).
5. J. D. Thomson and J. Brunet, *Trends Ecol. Evol.* **5**, 11 (1990).
6. D. G. Lloyd, *Genetica* **45**, 325 (1975).
7. B. Charlesworth and D. Charlesworth, *Am. Nat.* **112**, 975 (1978).
8. C. J. Webb, in (*3*), pp. 61–95.
9. H. G. Baker, *Cold Spring Harbor Symp. Quant. Biol.* **24**, 177 (1959).
10. D. Charlesworth, in *Evolution: Essays in Honour of John Maynard Smith*, P. J. Greenwood, P. H. Harvey, M. Slatkin, Eds. (Cambridge Univ. Press, Cambridge, 1985), pp. 237–268.
11. A. J. Richards, *Plant Breeding Systems* (Chapman & Hall, London, 1997).
12. D. de Nettancourt, *Incompatibility in Angiosperms* (Springer-Verlag, Berlin, 1977).
13. B. Chawla, R. Bernatzky, W. Liang, M. Marcotrigiano, *Theor. Appl. Genet.* **95**, 992 (1997).
14. J. Ramsey and D. W. Schemske, *Annu. Rev. Ecol. Syst.* **29**, 467 (1998).
15. B. C. Husband and D. W. Schemske, *Evolution* **51**, 737 (1997).
16. R. Lande and D. W. Schemske, *Evolution* **39**, 24 (1985).
17. J. Ronfort, *Genet. Res.* **74**, 31 (1999).
18. M. O. Johnston and D. J. Schoen, *Evolution* **48**, 1735 (1996).
19. D. R. Dewey, *Crop Sci.* **9**, 592 (1969).
20. H. G. Baker, *Am. Nat.* **124**, 149 (1984).
21. The internal transcribed spacers (ITS-1 and ITS-2) and the 5.8*S* cistron of nuclear ribosomal DNA were sequenced for 13 North American *Lycium* species, two *Grabowskia* species, and *Jaborosa integrifolia* following work by J. Wen and E. A. Zimmer [*Mol. Phylogenet. Evol.* **6**, 167 (1996)]. Sequences for *Grabowskia glauca* and four *Nolana* species were obtained from GenBank (accession numbers AB019954, AB019294, AB019311, AB019971, AB019314, AB019974, AB019966, AB019306, AB019289, and AB019949), and a sequence for *Atropa belladonna* was supplied by R. G. Olmstead. Sequences were aligned manually and combined with 29 morphological characters, producing a matrix of 733 characters, of which 17% were potentially phylogenetically informative. Phylogenies were inferred from 1000 random-addition sequence replicates with tree bisection reconnection (TBR) branch swapping using heuristic parsimony in PAUP* [D. L. Swofford, *Phylogenetic Analysis Using Parsimony (*and Other Methods)*, version 4.0b3a (Sinauer Associates, Sunderland, MA, 2000)]. Five hundred bootstrap searches, each with 50 random-addition sequence replicates and TBR branch swapping, were performed to assess the internal consistency of the data set. DNA sequences of this study are under GenBank accession numbers AF238981 through AF238995.
22. F. Chiang-Cabrera, dissertation, University of Texas, Austin (1981).
23. A. D. Richman and J. R. Kohn, *Plant Mol. Biol.* **42**, 169 (2000).
24. A. D. Richman, M. K. Uyenoyama, J. R. Kohn, *Science* **273**, 1212 (1996).
25. A. B. Stout and C. Chandler, *Science* **94**, 118 (1941).
26. J. S. Miller, in preparation.
27. A. M. Venter, H. J. T. Venter, R. L. Verhoeven, poster presented at the XVI International Botanical Congress, St. Louis, MO, 1 to 7 August 1999.
28. J. Masterson, *Science* **264**, 421 (1994).
29. Supplemental web material is available at www.sciencemag.org/feature/data/1053236.shl.
30. J. A. McComb, *Aust. J. Bot.* **16**, 525 (1968).

31. We thank L. McDade, J. Jaenike, R. Levin, and M. Nachman for comments on the manuscript and R. G. Olmstead for genomic DNAs (*Jaborosa integrifolia* and two species of *Grabowskia*) and a sequence for *Atropa belladonna*. This work was supported by grants from NSF (J.S.M. and D.L.V.), the University of Arizona Research Training Grant (J.S.M.), and Sigma Xi (J.S.M.).

16 June 2000; accepted 15 August 2000

Alteration of Stimulus-Specific Guard Cell Calcium Oscillations and Stomatal Closing in *Arabidopsis det3* Mutant

Gethyn J. Allen,[1]* Sarah P. Chu,[1]† Karin Schumacher,[2]†‡ Chad T. Shimazaki,[1] Dionne Vafeados,[2] Andrea Kemper,[3] Scott D. Hawke,[3] Gary Tallman,[3] Roger Y. Tsien,[4] Jeffrey F. Harper,[5] Joanne Chory,[2] Julian I. Schroeder[1]*

Cytosolic calcium oscillations control signaling in animal cells, whereas in plants their importance remains largely unknown. In wild-type *Arabidopsis* guard cells abscisic acid, oxidative stress, cold, and external calcium elicited cytosolic calcium oscillations of differing amplitudes and frequencies and induced stomatal closure. In guard cells of the V-ATPase mutant *det3*, external calcium and oxidative stress elicited prolonged calcium increases, which did not oscillate, and stomatal closure was abolished. Conversely, cold and abscisic acid elicited calcium oscillations in *det3*, and stomatal closure occurred normally. Moreover, in *det3* guard cells, experimentally imposing external calcium-induced oscillations rescued stomatal closure. These data provide genetic evidence that stimulus-specific calcium oscillations are necessary for stomatal closure.

Cytosolic calcium ($[Ca^{2+}]_{cyt}$) oscillations are an integral component of cell signaling, and the frequency, amplitude, and spatial localization of oscillations control the efficiency and specificity of cellular responses in animals (*1–3*). In plant cells $[Ca^{2+}]_{cyt}$ oscillations are induced by multiple stimuli (*4–9*); however, it remains unknown whether oscillations are required to elicit physiological responses in plants. Here we show that the *Arabidopsis det3* mutant abolishes guard cell $[Ca^{2+}]_{cyt}$ oscillations and stomatal closure in response to oxidative stress and extracellular calcium ($[Ca^{2+}]_{ext}$), but not to abscisic acid (ABA) and cold. Restoring $[Ca^{2+}]_{ext}$-induced $[Ca^{2+}]_{cyt}$ oscillations in *det3* guard cells rescued stomatal closure, suggesting that $[Ca^{2+}]_{cyt}$ oscillations are essential for stomatal closure.

Stomatal closure follows increases in guard cell $[Ca^{2+}]_{cyt}$ (*10*), and endomembrane calcium transport contributes to the $[Ca^{2+}]_{cyt}$ signal (*7*, *11–13*). Genetic impairment of endomembrane calcium transport could therefore provide a direct approach for dissecting $[Ca^{2+}]_{cyt}$ signals. The *de-etiolated 3* (*det3*) *Arabidopsis* mutant has reduced endomembrane energization owing to a 60% reduction

[1]Cell and Developmental Biology Section, Division of Biology and Center for Molecular Genetics, University of California, San Diego, La Jolla, CA 92093–0116, USA. [2]Howard Hughes Medical Institute and Plant Biology Laboratory, Salk Institute, 10010 North Torrey Pines Road, La Jolla, CA 92037–1099, USA. [3]Department of Biology, Willamette University, 900 State Street, Salem, OR 97301–3931, USA. [4]Department of Pharmacology and Chemistry and Biochemistry, Howard Hughes Medical Institute and Division of Cellular and Molecular Medicine, University of California, San Diego, La Jolla, CA 92093–0647, USA. [5]Department of Cell Biology, Scripps Research Institute, BCC283, 10550 North Torrey Pines Road, La Jolla, CA 92037, USA.

*To whom correspondence should be addressed. E-mail: gallen@biomail.ucsd.edu, julian@biomail.ucsd.edu

†These authors contributed equally to this work.

‡Present address: ZMBP-Pflanzenphysiologie, Universitaet Tuebingen, Auf der Morgenstelle 1, 72076 Tuebingen, Germany.

in expression of the C-subunit of the V-type H^+–adenosine triphosphatase (V-ATPase) (*14*). *det3* was identified by its failure to repress light-specific development in the dark; it has a dwarf phenotype, but normal stomatal development (*14*). Figure 1 shows *DET3* promoter–driven DET3–green fluorescent protein (GFP) fluorescence in *Arabidopsis* guard cells (Fig. 1A), protoplasts (Fig. 1C), and isolated vacuoles (Fig. 1D) and indicates that DET3 is expressed in guard cells and is localized on multiple membranes including both endoplasmic reticulum (ER) and vacuolar membranes. We hypothesized that endomembrane de-energization in *det3* guard cells could affect $[Ca^{2+}]_{cyt}$ signaling because Ca^{2+} sequestration into intracellular stores is H^+ gradient–dependent in many organisms (*15–19*).

Wild-type (WT) *Arabidopsis* stably expressing yellow cameleon 2.1 (YC2.1) under the control of the constitutive 35*S* promoter was used to measure $[Ca^{2+}]_{cyt}$ signals in stomatal guard cells (*20–22*). Oscillations in $[Ca^{2+}]_{cyt}$ were rapidly induced by 1 or 10 mM extracellular calcium in all 84 WT guard cells tested (Fig. 2, A and B). $[Ca^{2+}]_{cyt}$ oscillations were smaller and of higher frequency for 1 mM $[Ca^{2+}]_{ext}$ (average $[Ca^{2+}]_{cyt}$ at peak $\approx$ 160 nM; period = 161 $\pm$ 20 s) than for 10 mM $[Ca^{2+}]_{ext}$ ($[Ca^{2+}]_{cyt} \approx$ 1020 nM; period = 396 $\pm$ 23 s) [see also (*4*, *8*)]. Oscillations ceased after 45 to 60 min (Fig. 2B) and preceded maximal stomatal closure, which was measured after 3 hours. In *det3* guard cells, increasing $[Ca^{2+}]_{ext}$ from 0 to 1 or 10 mM caused immediate $[Ca^{2+}]_{cyt}$ increases which, unlike in the WT, subsequently failed to oscillate but consisted of small, rapid spikes superimposed on prolonged $[Ca^{2+}]_{cyt}$ increases (n = 55 of 56 cells) (Fig. 2, C and D) ($[Ca^{2+}]_{cyt} \approx$ 350 nM for 1 mM $[Ca^{2+}]_{ext}$ and $\approx$ 1250 nM for 10 mM $[Ca^{2+}]_{ext}$). Additionally, the total integrated $[Ca^{2+}]_{cyt}$ increase over an $\approx$30-min period was higher in *det3* [5910 $\pm$ 785 nM·min (n = 6)] than in WT [3010 $\pm$ 263 nM·min (n = 6)] at 10 mM $[Ca^{2+}]_{ext}$.

The absence of $[Ca^{2+}]_{ext}$-induced $[Ca^{2+}]_{cyt}$ oscillations in *det3* guard cells was consistent with a marked effect on $[Ca^{2+}]_{ext}$-induced stomatal closure. Addition of $[Ca^{2+}]_{ext}$ to preopened WT stomata caused closure, whereas in *det3* stomatal closure was abolished at all $[Ca^{2+}]_{ext}$ concentrations tested (Fig. 2E).

To further investigate the role of $[Ca^{2+}]_{cyt}$ oscillations and *det3* in guard cell signaling, we measured $[Ca^{2+}]_{cyt}$ and stomatal movements in response to other stimuli. In WT guard cells ABA caused repetitive $[Ca^{2+}]_{cyt}$ transients (Fig. 3A), or more prolonged oscillations (Fig. 3B), with a magnitude of $\sim$500 nM and a period of 468 $\pm$ 41 s (n = 40) for transients and 333 $\pm$ 35 s (n = 6) for oscillations (Fig. 3, A and B). In *det3*, ABA caused $[Ca^{2+}]_{cyt}$ transients or oscillations with near-identical magnitudes (Fig. 3, C and D) and periods (476 $\pm$ 32 s, n = 26 for transients and 328 $\pm$ 36 s, n = 4 for oscillations; $P > 0.15$ for WT versus *det3* periods for both transients and oscillations). ABA

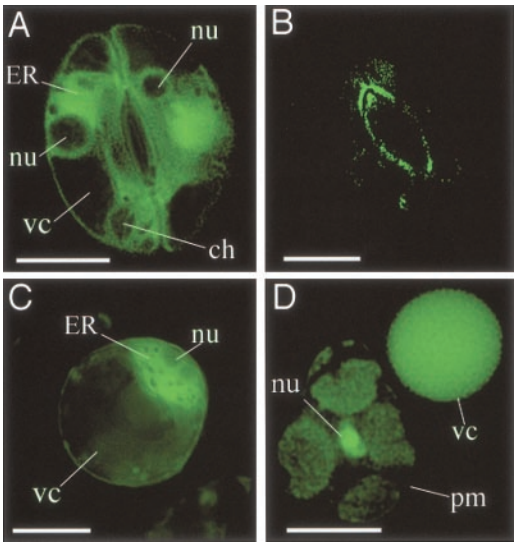

Fig. 1. Localization in *Arabidopsis* guard cells of a COOH-terminal DET3-GFP fusion expressed under the control of the DET3 promoter in plasmid pPZP221 (*14*). (**A**) GFP fluorescence is excluded from the vacuoles (vc), chloroplasts (ch), and nucleus (nu) and is concentrated in the ER. Bar, 5 μm. (**B**) Autofluorescence in nontransformed cell. Bar, 5 μm. (**C**) In guard cell protoplasts, GFP fluorescence is excluded from vacuoles (vc) and the nucleus (nu) and is concentrated in the ER. Bar, 4 μm. (**D**) In ruptured guard cell protoplasts fluorescence was associated with released vacuolar membranes (vc) and the collapsed nucleus (nu), but not the plasma membrane (pm). Bar, 4 μm.

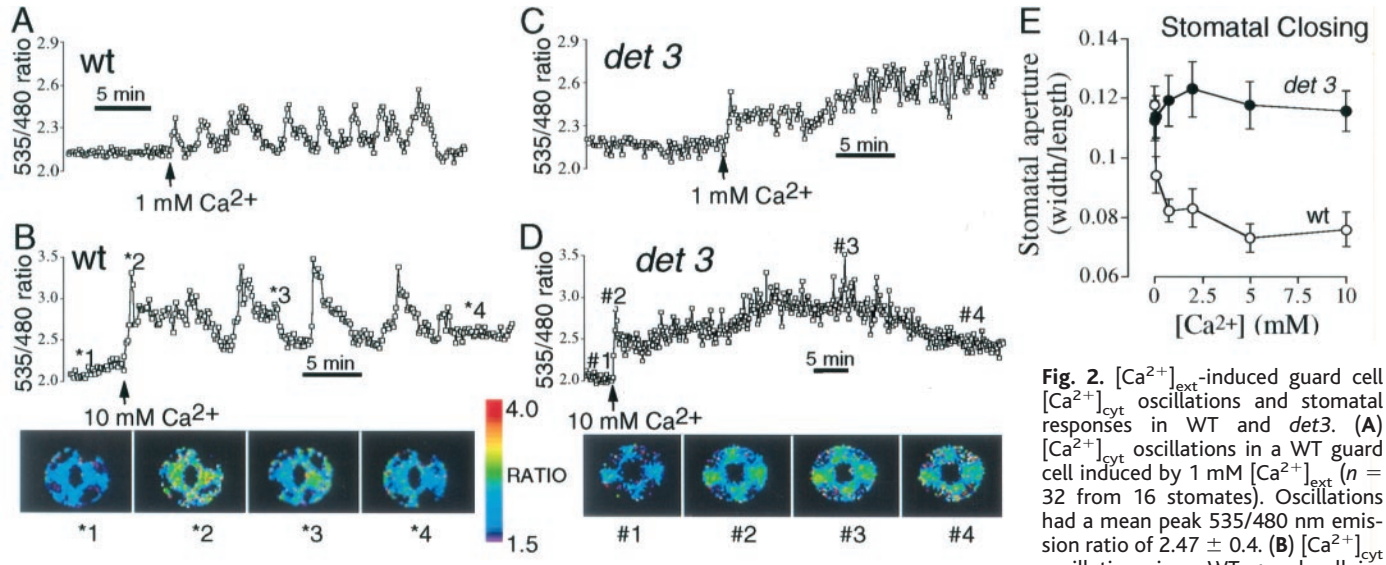

Fig. 2. $[Ca^{2+}]_{ext}$-induced guard cell $[Ca^{2+}]_{cyt}$ oscillations and stomatal responses in WT and *det3*. (**A**) $[Ca^{2+}]_{cyt}$ oscillations in a WT guard cell induced by 1 mM $[Ca^{2+}]_{ext}$ (n = 32 from 16 stomates). Oscillations had a mean peak 535/480 nm emission ratio of 2.47 $\pm$ 0.4. (**B**) $[Ca^{2+}]_{cyt}$ oscillations in a WT guard cell induced by 10 mM $[Ca^{2+}]_{ext}$ (n = 52 from 26 stomates). Oscillations had a mean peak 535/480 nm ratio of 3.21 $\pm$ 0.16. The trace is from the right-hand cell of the stomate in the lower panel. Images indicate the 535/480 nm ratio at points *1 to *4. (**C**) Increase of *det3* guard cell $[Ca^{2+}]_{cyt}$ induced by 1 mM $[Ca^{2+}]_{ext}$ (n = 21 cells from 11 stomates). Increases had a mean peak 535/480 nm ratio of 2.83 $\pm$ 0.31. (**D**) Increase of *det3* guard cell $[Ca^{2+}]_{cyt}$ induced by 10 mM extracellular calcium (n = 34 from 17 stomates). Increases had a mean peak 535/480 nm ratio of 3.26 $\pm$ 0.39. The trace is from the right-hand cell of the stomate in the lower panel. Images indicate the 535/480 nm ratio at points #1 to #4. (**E**) Increasing $[Ca^{2+}]_{ext}$ caused stomatal closure in WT (○) but not *det3* (●). Data are the mean $\pm$ SEM of 120 stomata from four replicates for each $[Ca^{2+}]_{ext}$.

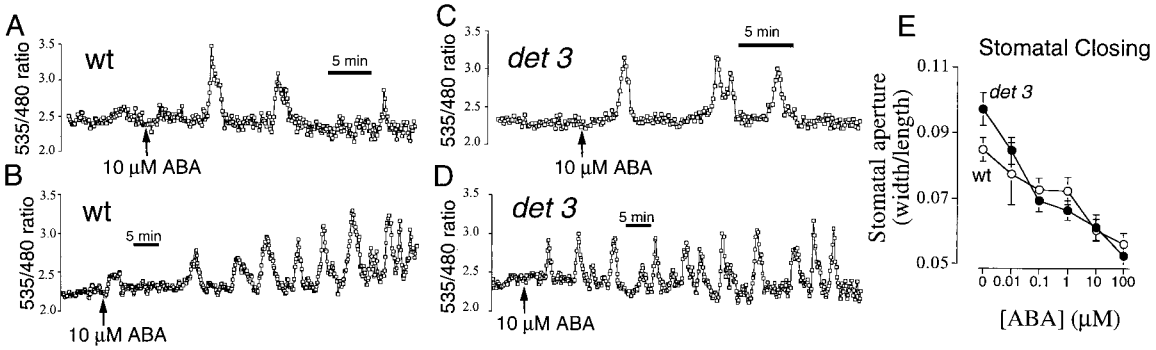

Fig. 3. ABA-induced guard cell $[Ca^{2+}]_{cyt}$ oscillations and stomatal responses in WT and *det3*. (**A**) Repetitive, transient $[Ca^{2+}]_{cyt}$ increases in a WT guard cell induced by 10 μM ABA (n = 40 from 28 stomates). Transients had a mean peak 535/480 nm ratio of 3.07 ± 0.29. (**B**) Oscillations of WT guard cell $[Ca^{2+}]_{cyt}$ induced by 10 μM ABA (n = 6 from three stomates). Oscillations had a mean peak 535/480 nm ratio of 2.91 ± 0.31. (**C**) Repetitive, transient increases in *det3* guard cell $[Ca^{2+}]_{cyt}$ induced by 10 μM ABA (n = 26 from 15 stomates). Transients had a mean peak 535/480 nm ratio of 3.09 ± 0.22. (**D**) Oscillations of *det3* guard cell $[Ca^{2+}]_{cyt}$ induced by 10 μM ABA (n = 4 from two stomates). Oscillations had a mean peak 535/480 nm ratio of 2.98 ± 0.31. Transients occurred in both guard cells of all responsive stomata (ABA-induced $[Ca^{2+}]_{cyt}$ increases were observed in 81% of cells, n = 76 from 96 stomates). (**E**) ABA induced stomatal closure in WT (○) and *det3* (●). Data are the mean ± SEM of 120 stomata from four replicates.

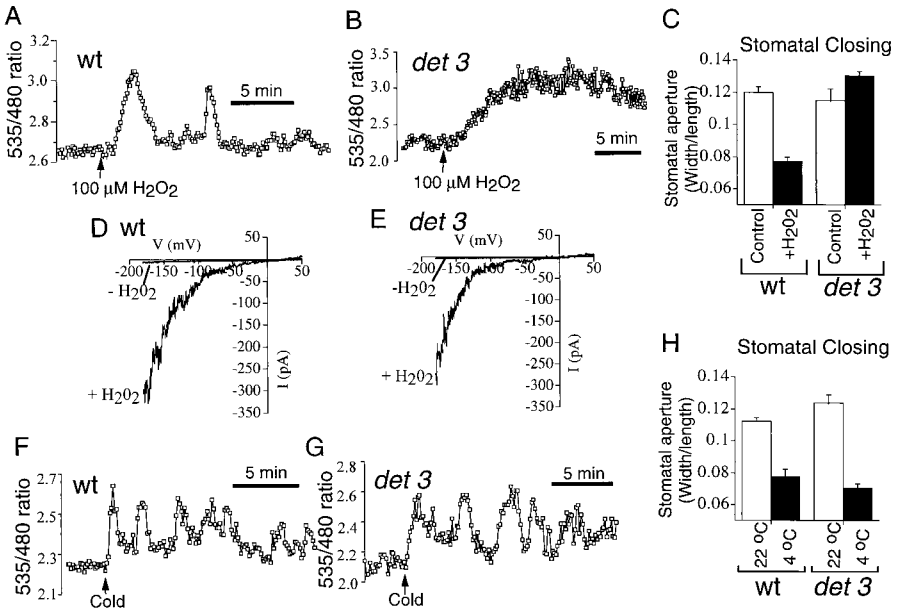

Fig. 4. Guard cell $[Ca^{2+}]_{cyt}$ oscillations and stomatal responses to H_2O_2 and cold in WT and *det3*. (**A**) Repetitive, transient increases in WT guard cell $[Ca^{2+}]_{cyt}$ induced by 100 μM H_2O_2 (n = 24 from 13 stomates). Transients had a mean peak 535/480 nm ratio of 3.11 ± 0.31 and a period, when two increases occurred, of 366 ± 31 s. (**B**) Increase of *det3* guard cell $[Ca^{2+}]_{cyt}$ induced by 100 μM H_2O_2 (n = 22 from 13 stomates). Increases had a mean peak 535/480 nm ratio of 3.31 ± 0.46. (**C**) One hundred micromolar H_2O_2 induced stomatal closure in WT (left bars) but not *det3* (right bars). Data are the mean ± SEM of 180 stomata from three replicates. Hyperpolarization activated calcium-permeable currents in (**D**) WT (n = 9) and (**E**) *det3* (n = 6) guard cell protoplasts induced by H_2O_2. (**F**) Oscillations of WT guard cell $[Ca^{2+}]_{cyt}$ induced by cold (n = 20 from 10 stomates). Oscillations had a mean peak 535/480 nm ratio of 2.66 ± 0.31. (**G**) Oscillations of *det3* guard cell $[Ca^{2+}]_{cyt}$ induced by cold (n = 18 from nine stomates). Oscillations had a mean peak 535/480 nm ratio of 2.61 ± 0.29. (**H**) Cold induced stomatal closure in WT (left) and *det3* (right). Data are the mean ± SEM of 180 stomata from three replicates.

also induced stomatal closure to the same extent in WT and *det3* (Fig. 3E).

Hydrogen peroxide (H_2O_2) also induced $[Ca^{2+}]_{cyt}$ increases in WT guard cells (*23*, *24*), consisting of one or two separate transients (Fig. 4A) with peak magnitudes of ~700 nM (n = 24). In *det3* guard cells H_2O_2 caused larger (≈1450 nM), more prolonged $[Ca^{2+}]_{cyt}$ increases (Fig. 4B, n = 22 cells), and H_2O_2-induced stomatal closure was abolished (Fig. 4C). H_2O_2-induced $[Ca^{2+}]_{cyt}$ signaling in guard cells requires activation of a plasma membrane calcium influx current (I_{Ca}) that shows enhanced activity at negative membrane potentials (*24*). Electrophysiological measurement (*22*) of I_{Ca} in guard cell protoplasts showed identical I_{Ca} activation by H_2O_2 in WT and *det3* (Fig. 4, D and E).

Cold increases plant cell $[Ca^{2+}]_{cyt}$ (*25*). In WT guard cells cold elicited small, repetitive $[Ca^{2+}]_{cyt}$ transients (amplitude ≈ 125 nM $[Ca^{2+}]_{cyt}$; frequency, 154 ± 11 s; n = 20 cells) (Fig. 4F). Cold-induced transients of similar amplitude and frequency (amplitude ≈ 125 nM $[Ca^{2+}]_{cyt}$; frequency, 162 ± 21 s; n = 18 cells) were measured in *det3* guard cells ($P < 0.01$) (Fig. 4G). Cold elicited stomatal closure to the same extent in *det3* and WT ($P < 0.05$) (Fig. 4H).

Calcium contents (predominantly vacuolar and ER) measured by elemental x-ray microanalysis (*26*) in intact guard cells of open stomates were indistinguishable between WT and *det3* (calcium as weight percent of total K^+, Na^+, and Ca^{2+} = 34.3 ± 1.2% for WT and 34.7 ± 0.7% for *det3*, n = 90 each). These data suggest that the residual 40% V-ATPase activity is sufficient to allow long-term intracellular calcium accumulation in *det3*. Therefore, disruption of $[Ca^{2+}]_{ext}$- and oxidative stress–induced $[Ca^{2+}]_{cyt}$ oscillations in *det3* guard cells (Figs. 2, C and D, and 4B) does not appear to be due to depletion of intracellular calcium stores.

The correlation in *det3* between stimuli for which guard cell $[Ca^{2+}]_{cyt}$ oscillations are disrupted and stomatal closure is abolished strongly suggests that $[Ca^{2+}]_{cyt}$ oscillations are necessary for stomatal closure. To critically test this hypothesis, we experimentally imposed $[Ca^{2+}]_{cyt}$ oscillations in guard cells using hyperpolarization-mediated calcium influx (*9*, *11*). Exchanging the bathing solution every 300 s between high-KCl (depolarizing) and low-KCl (hyperpolarizing) buffers (*22*), and adding $[Ca^{2+}]_{ext}$ concomitantly with the hyperpolarizing buffer, imposed repetitive $[Ca^{2+}]_{cyt}$ increases in WT guard cells (Fig. 5A, n = 20 cells) and resulted in stomatal closure (Fig. 5B, left panel, "Post Osc"). Removing external calcium with 10 mM EGTA prevented oscillations (n = 8) and inhibited stomatal closure when external K^+

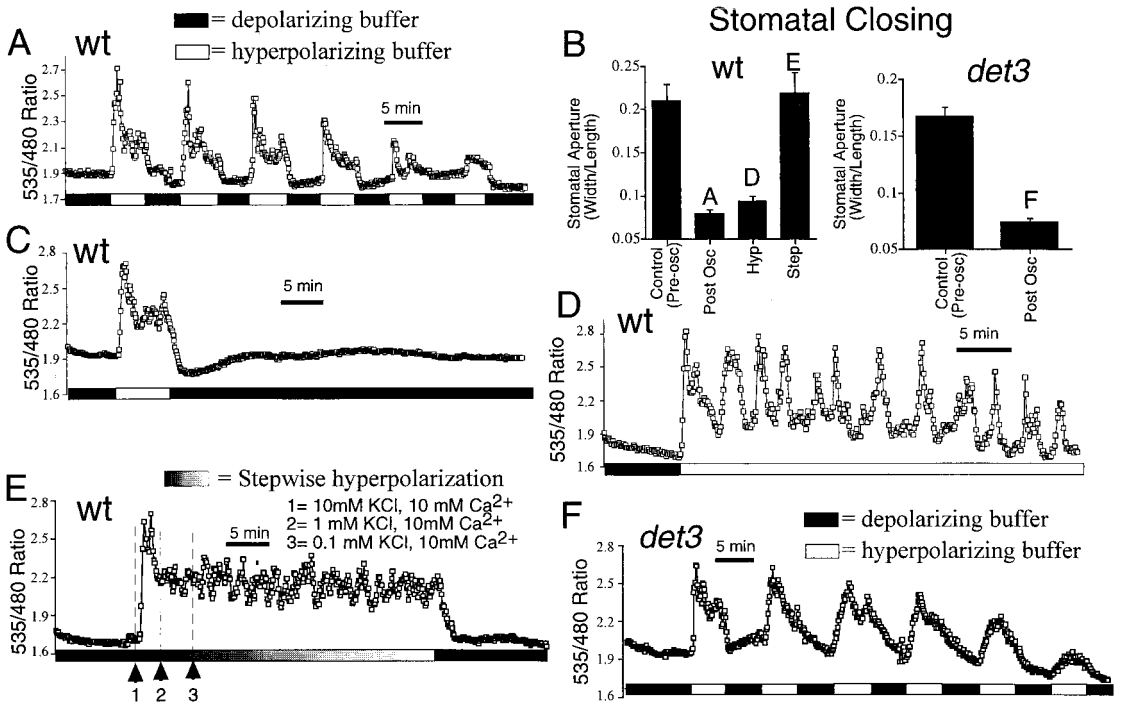

Fig. 5. Repetitive hyperpolarizations impose $[Ca^{2+}]_{cyt}$ oscillations in guard cells. (**A**) $[Ca^{2+}]_{cyt}$ oscillations in a WT guard cell resulting from exchanges between depolarizing (100 mM KCl, zero added Ca^{2+}) (■) and hyperpolarizing buffers (0.1 mM KCl, 10 mM Ca^{2+}) (□) (n = 20 from 10 stomates). (**B**) (Left) Inducing $[Ca^{2+}]_{cyt}$ oscillations close pre-opened [Control (Pre-osc)] stomata in WT (Post Osc). Oscillation-induced closure is elicited by continuous hyperpolarization (Hyp) but inhibited by prolonged $[Ca^{2+}]_{cyt}$ increase induced by stepwise hyperpolarization (Step). (Right) Oscillation-induced closure in *det3*. Data are the mean ± SEM of 160 stomata from four replicates. (**C**) One exchange from depolarizing to hyperpolarizing buffer (n = 12 from six stomates). (**D**) Continuous transfer to hyperpolarization buffer (n = 32 from 16 stomates). (**E**) A stepwise hyperpolarization induces prolonged $[Ca^{2+}]_{cyt}$ increases (n = 20 from 10 stomates). (**F**) Depolarizing to hyperpolarizing buffer exchanges as in (A) in *det3* guard cells (n = 18 from 11 stomates).

was repetitively exchanged (*27*). One 300-s hyperpolarization resulted in a single calcium transient, indicating that spontaneous oscillations were not initiated (Fig. 5C, n = 12 cells). Continuous transfer into the hyperpolarizing buffer (0.1 mM K^+) (Fig. 5D) induced oscillations with a higher frequency than oscillations induced by 10 mM $[Ca^{2+}]_{ext}$ at 5 mM K^+ [period = 178 ± 31 s, n = 32 compared with 396 ± 23 (Fig. 2B)] and resulted in stomatal closure (Fig. 5B, left panel, "Hyp"). However, imposing hyperpolarizations by decreasing external K^+ stepwise from 100 mM to 10, 1, and 0.1 mM, concomitant with the addition of 10 mM $[Ca^{2+}]_{ext}$, produced prolonged $[Ca^{2+}]_{cyt}$ increases in WT guard cells (Fig. 5E) similar to $[Ca^{2+}]_{ext}$-induced $[Ca^{2+}]_{cyt}$ increases in *det3* (compare Figs. 2, C and D, and 5E). Notably, prolonged $[Ca^{2+}]_{cyt}$ increases in WT also failed to elicit stomatal closure (Fig. 5B, left panel, "Step").

In *det3* guard cells, repetitive hyperpolarizations and the concomitant addition of 10 mM $[Ca^{2+}]_{ext}$ also induced $[Ca^{2+}]_{cyt}$ oscillations (Fig. 5F, n = 18 of 22 cells), which contrasted with the prolonged $[Ca^{2+}]_{cyt}$ increases induced by $[Ca^{2+}]_{ext}$ at constant external K^+ (Fig. 2, C and D). Remarkably, imposing $[Ca^{2+}]_{cyt}$ oscillations in *det3* guard cells elicited $[Ca^{2+}]_{ext}$-induced stomatal closure (Fig. 5B, right panel). Therefore, by restoring oscillations in *det3* guard cells, the impairment of $[Ca^{2+}]_{ext}$-induced stomatal closure was rescued.

The $[Ca^{2+}]_{cyt}$ oscillations elicited by ABA, cold, $[Ca^{2+}]_{ext}$, and oxidative stress had different amplitudes and frequencies (Figs. 2, A and B; 3, A and B; and 4, A and F), and all induced stomatal closure. Oscillations in $[Ca^{2+}]_{cyt}$ result from the interaction of three processes: extracellular calcium influx, intracellular calcium release, and sequestration into intracellular stores or across the plasma membrane (*28*, *29*). In guard cells the stimuli $[Ca^{2+}]_{ext}$ (*4*) and oxidative stress (*24*) activate calcium influx from the extracellular space. In *det3* guard cells these stimuli caused an initial $[Ca^{2+}]_{cyt}$ increase (Figs. 2, C and D, and 4B), suggesting that this initial calcium influx is unaffected, as also indicated by identical I_{Ca} activation in WT and *det3* (Fig. 4, D and E). However, in *det3* these stimuli caused prolonged $[Ca^{2+}]_{cyt}$ increases, suggesting that disruption of $[Ca_{2+}]_{cyt}$ oscillations is due to impaired endomembrane Ca^{2+} uptake. Disruption of endomembrane Ca^{2+} uptake in *det3* could occur by a number of possible mechanisms. Ca^{2+}/H^+ antiporter activity, which is involved in Ca^{2+} homeostasis in plant cells (*16*), may be reduced. Alternatively, a proposed direct facilitation of Ca^{2+}-ATPase activity by V-ATPases (*17*, *19*) might be disrupted in *det3*. Additionally, endomembrane lumen or cytosolic pH changes in *det3* may have effects on Ca^{2+} transporters.

Disruption of $[Ca^{2+}]_{cyt}$ oscillations in response to $[Ca^{2+}]_{ext}$ and oxidative stress but not ABA and cold suggests that different mechanisms generate oscillations for these stimuli. These mechanisms may involve different Ca^{2+} transporters located at separate intracellular calcium stores, as is found in animal cells (*18*, *19*), although certain components can be shared among stimuli (*9, 24, 25*).

In *det3* guard cells, the perfect correlation between those stimuli for which $[Ca^{2+}]_{cyt}$ oscillations were disrupted and stomatal closure was abolished strongly suggests that calcium oscillations are required for stomatal closure. Imposing oscillations rescued $[Ca^{2+}]_{ext}$-induced stomatal closure in *det3*, supporting previous hypotheses that calcium oscillations are required for physiological responses in guard cells (*30*). Prolonged $[Ca^{2+}]_{cyt}$ increases in *det3* (Fig. 2, C and D) or WT (Fig. 5, B and E) failed to elicit stomatal closure, suggesting, as in animal cells (*1–3*), that disruption of oscillations has a negative effect on some physiological responses. Therefore, regulation of the mechanism(s) in guard cells necessary to mediate stomatal closure is probably encoded by a pattern of periodic $[Ca^{2+}]_{cyt}$ increases. Overall, these findings strongly suggest that in *Arabidopsis* guard cells, $[Ca^{2+}]_{cyt}$ oscillations are essential to elicit stomatal closure.

References and Notes

1. W. Li, J. Llopis, M. Whitney, G. Zlokarnik, R. Y. Tsien *Nature* **392**, 936 (1998).
2. R. E. Dolmetsch, K. Xu, R. S. Lewis, *Nature* **392**, 933 (1998).
3. P. De Koninck and H. Schulman, *Science* **279**, 227 (1998).

4. M. R. McAinsh, A. A. R. Webb, J. E. Taylor, A. M. Hetherington, *Plant Cell* **7**, 1207 (1995).
5. D. W. Ehrhardt, R. Wais, S. R. Long, *Cell* **85**, 673 (1996).
6. T. L. Holdaway-Clarke *et al.*, *Plant Cell* **9**, 1999 (1997).
7. I. Staxén, C. Pical, L. T. Montgomery, J. E. Gray, A. M. Hetherington, *Proc. Natl. Acad. Sci. U.S.A.* **96**, 1779 (1999).
8. G. J. Allen, K. Kuchitsu, S. P. Chu, Y. Murata, J. I. Schroeder, *Plant Cell* **11**, 1785 (1999).
9. A. Grabov and M. R. Blatt, *Proc. Natl. Acad. Sci. U.S.A.* **95**, 4778 (1998).
10. M. R. McAinsh, C. Browlee, A. M. Hetherington, *Nature* **343**, 186 (1990).
11. S. Gilroy, N. D. Read, A. J. Trewavas, *Nature* **346**, 769 (1990).
12. C. P. Leckie, M. R. McAinsh, G. J. Allen, D. Sanders, D. A. M. Hetherington, *Proc. Natl. Acad. Sci. U.S.A.* **95**, 15837 (1998).
13. T. Jacob, S. Ritchie, S. M. Assmann, S. Gilroy, *Proc. Natl. Acad. Sci. U.S.A.* **96**, 12192 (1999).
14. K. Schumacher *et al.*, *Genes Dev.* **13**, 3259 (1999).
15. H. Sze, X. Li, M. G. Palmgren, *Plant Cell* **11**, 677 (1999).
16. K. D. Hirschi, *Plant Cell* **11**, 2113 (1999).
17. Y. Xie, M. B. Coukell, Z. Gombos, *J. Cell Sci.* **109**, 489 (1996).
18. C. Camello-Almaraz, J. A. Pariente, G. Salido, P. J. Camello, *Biochem. Res. Commun.* **271**, 311 (2000).
19. E. K. Rooney, J. D. Gross, M. Satre, *Cell Calcium* **16**, 509 (1994).
20. A. Miyawaki, O. Griesbeck, R. Heim, R. Y. Tsien, *Proc. Natl. Acad. Sci. U.S.A.* **96**, 2135 (1999).
21. G. J. Allen *et al.*, *Plant J.* **19**, 735 (1999).
22. $[Ca^{2+}]_{cyt}$ was measured (and calibrated in vitro) with YC2.1 as described (*21*) in 5 mM KCl, 10 mM MES-tris (pH 6.15). Ca^{2+} (50 μM) was added for experiments with ABA or H_2O_2. Epidermal strips were mounted on coverslips with medical adhesive (Hollister, Libertyville, IL). Aperture measurements were done as described (*8*, *21*) over a 3-hour period with the same buffers used for calcium imaging. To experimentally impose hyperpolarizations, we mounted epidermis in a 200-μl chamber and changed the perfusion buffer every 300 s between 100 mM KCl, zero $CaCl_2$, and 0.1 mM KCl, 10 mM $CaCl_2$. Aperture measurements were made in the same chamber before and after solution exchanges. WT and *det3* were treated simultaneously in blind assays in the same chamber. Guard cell protoplasts were prepared and recordings made by patch clamp as described (*24*) with barium as the charge carrier to analyze calcium currents. I_{Ca} activation by 5 mM H_2O_2 occurred in all cells.
23. M. R. McAinsh, H. Clayton, T. A. Mansfield, A. M. Hetherington, *Plant Physiol.* **111**, 1031 (1996).
24. Z. M. Pei *et al.*, *Nature* **406**, 731 (2000).
25. H. Knight, A. J. Trewavas, M. R. Knight, *Plant Cell* **8**, 489 (1996).
26. Epidermis (abaxial) was collected in the light by appressing leaves to carbon tabs (12 mm; Ted Pella, Redding, CA). Samples were washed in deionized water, frozen in liquid nitrogen, and stored for 48 to 72 hours at −20°C. Dried strips were warmed in a desiccator, sputter-coated with gold, and viewed with a scanning electron microscope. Guard cell ion contents were determined by x-ray elemental analysis with spectra from within cell wall perimeters (90 cells each for WT and *det3*, 30 from three separate leaves).
27. G. J. Allen *et al*., data not shown.
28. D. E. Clapham, *Cell* **80**, 259 (1995).
29. M. D. Bootman and M. J. Berridge, *Cell* **83**, 675 (1995).
30. M. R. McAinsh and A. M. Hetherington, *Trends Plant Sci.* **3**, 32 (1997).
31. We thank A. Webb (Cambridge, UK) for suggesting the medical adhesive. Supported by grants from NIH (R01 GM60396-01), NSF (MCB-9506191), and the U.S. Department of Energy (FG03-94-ER20148 to J.I.S. and FG03-94-ER20152 to J.F.H.); NSF (MCB9631390) and the Howard Hughes Medical Institute to J.C.; and MCB-9900525 to G.T.

5 June 2000; accepted 11 August 2000

High Direct Estimate of the Mutation Rate in the Mitochondrial Genome of *Caenorhabditis elegans*

Dee R. Denver,[1] Krystalynne Morris,[1] Michael Lynch,[2] Larissa L. Vassilieva,[2]* W. Kelley Thomas[1]†

Mutations in the mitochondrial genome have been implicated in numerous human genetic disorders and offer important data for phylogenetic, forensic, and population genetic studies. Using a long-term series of *Caenorhabditis elegans* mutation accumulation lines, we performed a wide-scale screen for mutations in the mitochondrial genome that revealed a mutation rate that is two orders of magnitude higher than previous indirect estimates, a highly biased mutational spectrum, multiple mutations affecting coding function, as well as mutational hotspots at homopolymeric nucleotide stretches.

Understanding the onset of mitochondrial disease and effective evolutionary analysis require accurate estimates of the rate and pattern of mitochondrial mutation, both of which have been the focus of recent controversy. Phylogenetic estimates of the substitution rate in the control region and protein-coding sequences of the human mitochondrial genome range from 0.02 to 0.26 per site per 10^6 years (My) (*1*, *2*). By contrast, pedigree analyses of the human control region and protein-coding sequences suggest that the substitution rate is much higher: ~2.5 per site per My (*3*, *4*). This discrepancy may be a consequence of mutational hotspots in the control region and/or the mitochondrial disease state of the individuals included in the pedigree analyses (*5*, *6*). Because the rate and pattern of mitochondrial substitution observed over phylogenetic time are a function of both the baseline mutational spectrum and its subsequent modification by natural selection, they likely provide a highly biased view of the rate and pattern of mutation. Unfortunately, almost all of our current estimates are based on indirect arguments and observations that may be biased by the consequences of selection (*7*, *8*).

A direct estimate of the mitochondrial mutation rate and pattern was accomplished by sequencing 10,428 base pairs (bp) of the mitochondrial genomes of 74 *Caenorhabditis elegans* mutation accumulation (MA) lines maintained for an average of 214 generations by single-progeny descent (*9*–*12*). Each MA line was propagated in a benign environment across generations by a single, random worm. This resulted in an effective population size of each MA line equal to one; hence, the efficiency of natural selection was reduced to a minimum, ensuring that all mutations, except those with extreme effects, accumulated over time in a neutral manner. These lines are known to have undergone a substantial decline in productivity, survival to maturity, generation time, and fitness as a consequence of deleterious-mutation accumulation (*12*).

Among the 74 MA lines, we analyzed 771,672 bp and observed 26 mutations for a total mutation rate equal to 1.6×10^{-7} per site per generation ($\pm 3.1 \times 10^{-8}$), or based on an average generation time of 4 days, 14.3 per site per My (±2.8). Sixteen of these mutations were base substitutions (Table 1), yielding a direct estimate of the mitochondrial mutation rate for base substitutions equal to 9.7×10^{-8} per site per generation ($\pm 2.4 \times 10^{-8}$), or 8.9 per site per My (±2.2). This observed rate is two orders of magnitude higher than the phylogenetic estimates discussed above and exceeds rates derived from pedigree analyses (*1*–*4*). The 16 base substitutions occurred across unique sites in 15 different MA lines, suggesting that the observed rate of base substitution is a product neither of hotspots nor of lines predisposed to mitochondrial mutation. Furthermore, the observed numbers of lines with 0, 1, and 2 mutations are nearly identical to those expected on the basis of a Poisson distribution (*13*).

Animal mitochondrial DNA (mtDNA) evolution is characterized by a strong bias toward transition (G↔A or T↔C) substitutions, but it has been unclear whether this phenomenon is a consequence of selection or of the baseline mutational spectrum (*14*, *15*). Comparison of two natural isolates of *C. elegans*, N2 (England) and RC301 (Germany), revealed 27 transitions and 2 transversions in mtDNA (*16*). Similarly,

[1]Division of Molecular Biology and Biochemistry, School of Biological Sciences, University of Missouri–Kansas City, Kansas City, MO 64110, USA. [2]Department of Biology, University of Oregon, Eugene, OR 97403, USA.

*Present address: Molecular and Cellular Biology Department, University of Arizona, Tucson, AZ 85721, USA.

†To whom correspondence should be addressed. E-mail: thomaske@umkc.edu